JOURNAL OF AGRICULTURAL AND FOOD CHEMISTRY

Pyrazole Derivatives as Photosynthetic Electron Transport Inhibitors: New Leads and Structure−Activity Relationship

CHIARA B. VICENTINI,[†] SALVATORE GUCCIONE,[#] LAURA GIURATO,[#] REBECCA CIACCIO,[#] DONATELLA MARES,[‡] AND GIUSEPPE FORLANI*[,§]

Dipartimento di Scienze Farmaceutiche, Dipartimento delle Risorse Naturali e Culturali, and Dipartimento di Biologia, Università di Ferrara, Italy; and Dipartimento di Scienze Farmaceutiche, Università di Catania, Italy

Four series of new pyrazoles, namely, 5 4-carboxypyrazolo-3-*tert*-butylcarboxamide and 6 4-carboxypyrazolo-3-cyclopropylcarboxamide derivatives and 10 pyrazolo[3,4-*d*][1,3]thiazine-4-one and 9 pyrazolo[3,4-*d*][1,3]thiazine-4-thione derivatives, were synthesized and screened as potential inhibitors of photosynthetic electron transport. The structures were confirmed by ^{1}H NMR, elemental, and IR analyses. Their biological activity was evaluated in vitro as the ability to interfere with the light-driven reduction of ferricyanide by isolated spinach chloroplasts. Only a few compounds exhibited excellent inhibitory properties in the micromolar range, comparable to those of commercial herbicides sharing the same target, such as diuron, lenacil, and hexazinone. Nevertheless, most of the remaining molecules exerted a remarkable inhibition in the millimolar range. Combined with previous results on 6 pyrazolo[1,5-*a*][1,3,5]triazine-2,4-dione and 4 pyrazolo[1,5-*c*][1,3,5]thiadiazine-2-one derivatives, these data allowed a comprehensive analysis of structure−activity relationship. Molecular modeling studies were undertaken to rationalize the structural determinants of activity in terms of shape, size, and molecular fields. Results suggested that the inhibitory potential of these compounds is associated mainly with their electrostatic properties.

KEYWORDS: Herbicides; photosynthetic electron transport inhibitors; pyrazole derivatives; structure−activity relationship

INTRODUCTION

Several reasons exist today for developing new weed control systems. Pesticides should have a favorable combination of properties, such as high specific activity, low application rates, crop tolerance, and low mammalian toxicity. Increasing public concern for environmental pollution derived from agricultural practices also requires that herbicides be rapidly degraded by soilborne microorganisms. Moreover, during the past decade, intensive and repeated applications of the same active ingredients caused the selection for and development of herbicide resistance (*1*). In most cases, resistance is due to an altered target site (*2*). Herbicide-resistant weeds often show a wide pattern of cross-resistance to both structurally similar herbicides and other phytochemicals sharing the same target (*3*). Intensive efforts have thus been undertaken to discover new compounds with favorable environmental and safety features to selectively control weeds. Recently, this aim has been pursued with new strategies, switching from the evaluation of in planta herbicidal efficacy to target-based in vitro assays (*4*, *5*).

Many pyrazole derivatives with promising herbicidal properties have been discovered. Among the active principles already introduced in the agricultural practice are the inhibitor of protoporphyrinogen oxidase pyraflufen-ethyl (HRAC group E) (*6*), the bleaching herbicides pyrazolynate, pyrazoxyfen, and benzofenap, which act through the inhibition of 4-hydroxyphenylpyruvate dioxygenase (HRAC group F2), the branched-chain amino acid inhibitors, the sulfonylureas halosulfuron-methyl, pyrazosulfuron-ethyl, and azimsulfuron (HRAC group B), the inhibitor of cell division, metazachlor (HRAC group K3), and the unknown target herbicide difenzoquat (HRAC group Z). Moreover, pyrimidine-2,4-dione derivatives, including uracils such as lenacil, terbacil, bromacil, and 1,3,5-triazine-2,4-dione derivatives, including the triazolinone hexazinone, have been characterized as photosynthetic electron transport inhibitors (HRAC group C1) (*4*, *5*).

A large number of herbicides act by inhibiting chloroplast electron transport. In most cases the molecular target was found to be the plastoquinone-binding site on the D1 protein in the photosystem II (PSII) reaction center (*7*). Tight binding to this domain leads to a block in NADPH production, which is required for CO_2 fixation. This, in turn, induces the formation

* Author to whom correspondence should be addressed [fax (39)0532-249761; e-mail flg@unife.it].
[†] Dipartimento di Scienze Farmaceutiche, via Fossato di Mortara 17−19, Ferrara.
[#] Dipartimento di Scienze Farmaceutiche, v.le A. Doria 6, Ed. 2, Catania.
[‡] Dipartimento delle Risorse Naturali e Culturali, c.so Porta Mare 2, Ferrara.
[§] Dipartimento di Biologia, via L. Borsari 46, Ferrara, Italy.

10.1021/jf0500029 CCC: $30.25
Published on Web 04/21/2005

Scheme 1

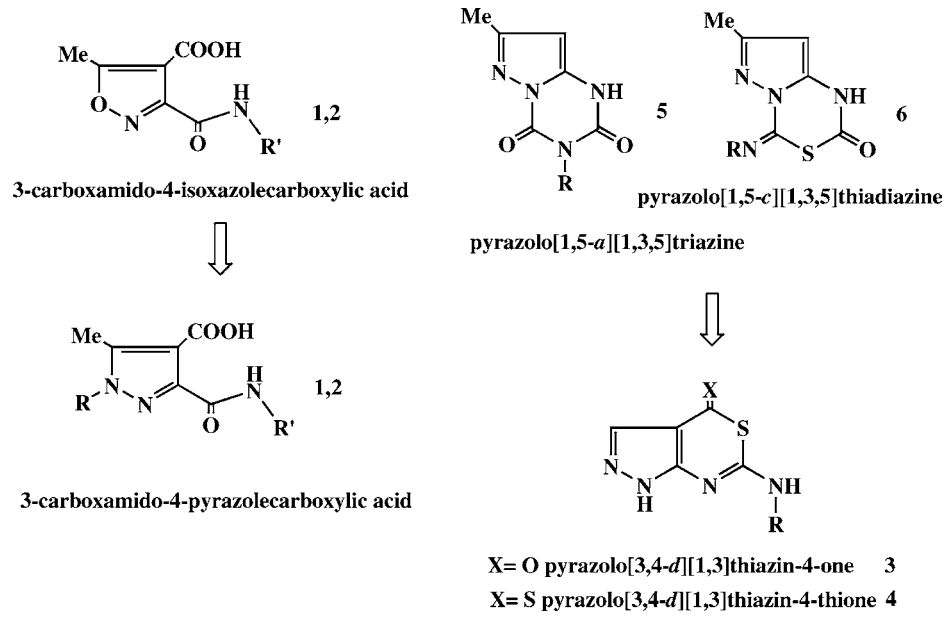

of free oxygen radicals, which cause photooxidation of chlorophylls and lipids, thus breaking down thylakoid integrity, which is strictly required for chloroplast functionality (*8*). A renewed interest in the development of further compounds sharing this mode of action is witnessed by numerous papers recently published on this subject. A group of 3-carboxamido-4-isoxazolecarboxylic acids (**1** and **2**) (**Scheme 1**) was found to exhibit herbicidal properties, and some of them in the micromolar range were able to inhibit the Hill reaction of thylakoids from wheat (*9*). Herbicidal amino- and urea-substituted thiazoles also appear to act via PSII interference. Their relative inhibitory activity showed that lipophilicity, as modulated by the length of the hydrocarbon side chain, has a great impact on in vitro effectiveness. Isopropyl and *n*-butyl side chains conferred maximal activity, and this was interpreted as a steric requirement to reach the Q_B binding site in the thylakoidal membrane. However, some discrepancies were found between the results of in vitro and in vivo tests (*10*). Also, in the case of herbicidal 2-hydroxy-3-alkyl-1,4-naphthoquinones the length of the 3-*n*-alkyl substituent for optimal activity differed between in planta and in vitro activities (*11*). Both 2-cyano-3-substituted-pyridinemethylaminoacrylates (*12*) and 2-cyano-3-(2-chlorothiazol-5-yl)methylaminoacrylates (*13*), some of which showed excellent herbicidal activities at doses as low as 75 g ha^{-1}, were found to inhibit PSII electron transport. In a previous paper, we also reported on some pyrazolo[1,5-*a*][1,3,5]triazine-2,4-dione (**5**) and pyrazolo[1,5-*c*][1,3,5]thiadiazine-2-one (**6**) derivatives that exhibited remarkable inhibitory properties at the PSII level, comparable to those of the reference commercial herbicides lenacil, diuron, and hexazinone (*14*).

Until recently, a structure−activity relationship analysis that allowed a rational molecular design of new PSII-inhibiting herbicides by structure modeling was limited because a sufficiently high-resolution X-ray structure of photosystem II was not available. The reaction center of purple photosynthetic bacteria, which is homologous to PSII, served as a model, but increasing evidence showed that there is significant variation between the two Q_B sites. However, the structure of PSII of the cyanobacterium *Thermosynechococcus elongatus* has been recently described at 3.5 Å resolution, revealing its molecular architecture and details of the binding sites for cofactors (*15*). This result opens up highly interesting prospects of developing new active principles. In this view, a re-evaluation of those compounds that had previously shown an ability to interfere with the photosynthetic electron transport chain may also provide researchers with useful information.

Here we report the synthesis of some pyrazolo[3,4-*d*][1,3]-thiazin-4-one/thione derivatives (**3** and **4**) and the screening for the ability to inhibit the Hill reaction in isolated spinach chloroplasts of compounds **1**−**4**, in comparison with those compounds already synthesized and tested (**5** and **6**) (*14*). Results, combined with previous data and supported by molecular modeling, allowed us a thorough analysis of structure−activity relationships. This led to the definition of molecular properties, in terms of shape, electronics, and hydrophobic complementarity to the macromolecular site, which are required for the design and synthesis of new active principles.

MATERIALS AND METHODS

Chemicals. Melting points were determined with a Buchi capillary apparatus and are uncorrected. IR spectra were recorded with a Perkin-Elmer Paragon 500 FT-IR spectrometer using potassium bromide pellets. ^{1}H NMR spectra were recorded on a Bruker AC200 spectrometer; chemical shifts (δ) are given in parts per million relative to the tetramethylsilane as internal standard. Yields were based on the weight of the products dried in vacuo over phosphorus pentoxide. Elemental analyses (C, H, N, S) were within ±0.4 of theoretical values. Column chromatography was performed using silica gel (70−230 mesh); for the flash chromatography technique, silica gel (230−400 mesh) was employed.

Synthesis. The 3-carboxamido-4-pyrazolecarboxylic acid (**1n**−**r**, **2n**−**s**) and 3-carboxamido-4-isoxazolecarboxylic acid (**1m**, **2m**) (*16*, *17*) and the pyrazolo[1,5-*a*][1,3,5]triazine-2,4-dione (**5e**−**l**) and the pyrazolo[1,5-*c*][1,3,5]thiadiazine-2-one (**6g**−**j**) (*14*) derivatives were prepared according to previously reported procedures.

*N-Alkyl/aryl-N′-(4-carboethoxy-3-pyrazolyl)thioureas (**8a**−**j**).* A mixture of 3-amino-4-carboethoxypyrazole **7** (3.10 g, 20 mmol) and the appropriate isothiocyanate in toluene (20 mL) was heated under reflux for 6 h and then cooled. *N*-Substituted-*N′*-(4-carboethoxy-3-pyrazolyl)-thioureas **8a**−**f**,**i** precipitated spontaneously and were collected as pure products. After removal of solvent, the residue was shown to be a mixture of products, and *N′*-(3-pyrazolyl) thioureas **8g**,**h**,**j** were isolated after purification by silica gel chromatography as byproducts.

By using this procedure the following compounds were obtained:

***8a** (R = 3-trifluoromethylphenyl):* yield, 75%; mp, 169.3−169.7 °C; IR (KBr, cm^{-1}), ν_{max} 3351, 1666, 1589, 1534; ^{1}H NMR (DMSO-d_6), δ

1.30 (t, 3H, Me, $J = 7.2$ Hz), 4.29 (q, 2H, CH_2, $J = 7.2$ Hz), 7.61−8.15 (m, 4H, Ph), 8.45 (s, 1H, CH), 9.61 (s, 1H, NH), 11.55 (s, 1H, NH), 13.53 (s, 1H, NH).

8b *(R = 4-bromophenyl):* yield, 87%; mp, 211−213.8 °C; IR (KBr, cm^{-1}), ν_{max} 3220, 1663, 1575, 1539; ^1H NMR (DMSO-d_6), δ 1.30 (t, 3H, Me, $J = 7.2$ Hz), 4.29 (q, 2H, CH_2, $J = 7.2$ Hz), 7.56−7.62 (m, 4H, Ph), 8.45 (s, 1H, CH), 9.54 (s, 1H, NH), 11.45 (s, 1H, NH), 13.51 (s, 1H, NH).

8c *(R = 4-chlorophenyl):* yield, 78%; mp, 194−196 °C; IR (KBr, cm^{-1}), ν_{max} 3220, 1662, 1575, 1537; ^1H NMR (DMSO-d_6), δ 1.30 (t, 3H, Me, $J = 7.0$ Hz), 4.30 (q, 2H, CH_2, $J = 7.0$ Hz), 7.44−7.70 (m, 4H, Ph), 8.45 (s, 1H, CH), 9.54 (s, 1H, NH), 11.45 (s, 1H, NH), 13.51 (s, 1H, NH).

8d *(R = 3-chlorophenyl):* yield, 84%; mp, 183.5−184.2 °C; IR (KBr, cm^{-1}), ν_{max} 3272, 1660, 1583, 1537; ^1H NMR (DMSO-d_6), δ 1.30 (t, 3H, Me, $J = 7.2$ Hz), 4.30 (q, 2H, CH_2, $J = 7.2$ Hz), 7.28−7.90 (m, 4H, Ph), 8.45 (s, 1H, CH), 9.56 (s, 1H, NH), 11.50 (s, 1H, NH), 13.53 (s, 1H, NH).

8e *(R = 2-chlorophenyl):* yield, 80%; mp, 173.8−176 °C; IR (KBr, cm^{-1}), ν_{max} 3275, 1656, 1587, 1539; ^1H NMR (DMSO-d_6), δ 1.31 (t, 3H, Me, $J = 7.2$ Hz), 4.30 (q, 2H, CH_2, $J = 7.2$ Hz), 7.60−8.10 (m, 4H, Ph), 8.46 (s, 1H, CH), 9.63 (s, 1H, NH), 11.49 (s, 1H, NH), 13.56 (s, 1H, NH).

8f *(R = 4-nitrophenyl):* yield, 98%; mp, 211−213 °C; IR (KBr, cm^{-1}), ν_{max} 3247, 1656, 1595, 1539; ^1H NMR (DMSO-d_6), δ 1.30 (t, 3H, Me, $J = 7.2$ Hz), 4.28 (q, 2H, CH_2, $J = 7.2$ Hz), 8.02−8.30 (m, 4H, Ph), 8.45 (s, 1H, CH), 9.71 (s, 1H, NH), 11.73 (s, 1H, NH), 13.56 (s, 1H, NH).

8g *(R = ethyl):* yield, 8%; mp, 133 °C (purified by column chromatography; eluent, ethyl acetate/petroleum ether, 3:7, 8:2; IR (KBr, cm^{-1}), ν_{max} 3244, 1659, 1578, 1539; ^1H NMR (DMSO-d_6), δ 1.16−1.33 (m, 6H, 2Me), 3.58−3.64 (m, 2H, CH_2,), 4.27 (q, 2H, CH_2, $J = 7.2$ Hz), 8.38 (s, 1H, CH), 9.25 (s, 1H, NH), 9.66 (br t, 1H, NH), 13.33 (s, 1H, NH).

8h *(R = butyl):* yield, 7%; mp, 100−102 °C (purified by column chromatography; eluent, ethyl acetate/petroleum ether, 2:8, 3:7, 8:2); IR (KBr, cm^{-1}), ν_{max} 3247, 1663, 1588, 1540; ^1H NMR (DMSO-d_6), δ 0.91 (t, 3H, Me, $J = 7.2$ Hz), 1.24−1.62 (m, 7H, Me + $2CH_2$), 3.55−3.64 (m, 2H, CH_2), 4.27 (q, 2H, CH_2, $J = 7.2$ Hz), 8.38 (s, 1H, CH), 9.26 (s, 1H, NH), 9.71 (t, 1H, NH, $J = 5.1$ Hz), 13.34 (s, 1H, NH).

8i *(R = benzyl):* yield, 40%; mp, 184.3−191.2 °C; IR (KBr, cm^{-1}), ν_{max} 3289, 1656, 1625, 1583, 1542; ^1H NMR (DMSO-d_6), δ 1.29 (t, 3H, Me, $J = 7.0$ Hz), 4.27 (q, 2H, CH_2, $J = 7.0$ Hz), 4.87 (d, 2H, CH_2, $J = 5.6$ Hz), 7.30−7.37 (m, 5H, Ph), 8.37 (s, 1H, CH), 9.38 (s, 1H, NH), 10.04 (t, 1H, NH, $J = 5.4$ Hz), 13.32 (s, 1H, NH).

8j *(R = cyclohexyl):* yield, 8%; mp, 141−141.6 °C (purified by column chromatography, eluent ethyl acetate/petroleum ether, 3:7, 8:2); IR (KBr, cm^{-1}), ν_{max} 3244, 2931, 1669, 1585, 1539; ^1H NMR (DMSO-d_6), δ 1.25−1.98 (m, 13H, Me + cyclohexyl), 4.13 (m, 1H, CH, cyclohexyl), 4.27 (q, 2H, CH_2, $J = 7.2$ Hz), 8.38 (s, 1H, CH), 9.22 (s, 1H, NH), 9.74 (d, 1H, NH, $J = 7.8$ Hz), 13.36 (s, 1H, NH).

*Synthesis of 6-Substituted Pyrazolo[3,4-d][1,3]thiazin-4-ones (**3a**−**j**).* A solution of **8** (0.6 g) in 98% sulfuric acid (4 mL) was stirred at room temperature for 4 days and then poured into ice water. The precipitate was collected and purified by column chromatography, eluent ethyl acetate/petroleum ether 1:1.

By using this procedure the following compounds were obtained:

3a *(R = 3-trifluoromethylphenyl):* yield, 80%; mp, 239−241 °C; IR (KBr, cm^{-1}), ν_{max} 3095, 1669, 1557; ^1H NMR (DMSO-d_6), δ 7.46−8.07 (m, 4H, Ph), 8.17 (s, 1H, CH), 10.87 (br, 1H, NH), 13.75 (br, 1H, NH).

3b *(R = 4-bromophenyl):* yield, 80%; mp, 253−255 °C; IR (KBr, cm^{-1}), ν_{max} 3406, 3312, 1658, 1608, 1560, 1531; ^1H NMR (DMSO-d_6), δ 7.52−7.75 (m, 4H, Ph), 7.97 (s, 1H, CH), 10.66 (br, 1H, NH), 13.66 (br, 1H, NH).

3c *(R = 4-chlorophenyl):* yield, 79%; mp, 223−225 °C; IR (KBr, cm^{-1}), ν_{max} 3056, 1669, 1538; ^1H NMR (DMSO-d_6), δ 7.41−7.82 (m, 4H, Ph), 8.04 (s, 1H, CH), 10.64 (br, 1H, NH), 13.63 (br, 1H, NH).

3d *(R = 3-chlorophenyl):* yield, 98%; mp, 241−243 °C; IR (KBr, cm^{-1}), ν_{max} 3069, 1673, 1567, 1541; ^1H NMR (DMSO-d_6), δ 7.14−7.62 (m, 4H, Ph), 7.96 (s, 1H, CH), 10.70 (br, 1H, NH), 13.69 (br, 1H, NH).

3e *(R = 2-chlorophenyl):* yield, 76%; mp, 213−215 °C; IR (KBr, cm^{-1}), ν_{max} 3071, 1693, 1560, 1531; ^1H NMR (DMSO-d_6), δ 7.35−7.62 (m, 4H, Ph), 7.92 (s, 1H, CH), 10.50 (br, 1H, NH), 13.52 (br, 1H, NH).

3f *(R = 4-nitrophenyl):* yield, 39%; mp, 208−210 °C; IR (KBr, cm^{-1}), ν_{max} 3401, 3312, 1662, 1537, 1495; ^1H NMR (DMSO-d_6), δ 8.01−8.27 (m, 4H, Ph), 8.15 (s, 1H, CH), 11.06 (br, 1H, NH), 13.70 (br, 1H, NH).

3g *(R = ethyl):* yield, 70%; mp, 246−249.7 °C; IR (KBr, cm^{-1}), ν_{max} 3310, 1672, 1574, 1544; ^1H NMR (DMSO-d_6), δ 1.16 (t, 3H, Me, $J = 7.2$ Hz), 3.34−3.46 (m, 2H, CH_2), 7.86 (s, 1H, CH), 8.66 (br, 1H, NH), 13.33 (br, 1H, NH).

3h *(R = butyl):* yield, 87%; mp, 175.7−177.3 °C; IR (KBr, cm^{-1}), ν_{max} 3312, 1660, 1542; ^1H NMR (DMSO-d_6), δ 0.89 (t, 3H, Me, $J = 7.2$ Hz), 1.30−1.58 (m, 4H, $2CH_2$), 3.32−3.42 (m, 2H, CH_2), 7.86 (s, 1H, CH), 8.65 (br, 1H, NH), 13.25 (br, 1H, NH).

3i *(R = benzyl):* yield, 30%; mp, 154.3−155.9 °C; IR (KBr, cm^{-1}), ν_{max} 3192, 1677, 1551; ^1H NMR (DMSO-d_6), δ 4.60 (d, 2H, CH_2, $J = 5.8$ Hz), 7.23−7.35 (m, 5H, Ph), 7.86 (s, 1H, CH), 9.19 (br, 1H, NH), 13.34 (br, 1H, NH).

3j *(R = cyclohexyl):* yield, 84%; mp, 169.4 °C; IR (KBr, cm^{-1}), ν_{max} 3254, 2930, 1724, 1645; ^1H NMR (DMSO-d_6), δ 1.10−1.92 (m, 10H, cyclohexyl), 3.89 (m, 1H, cyclohexyl), 7.84 (s, 1H, CH), 8.55 (d, 1H, NH, $J = 7.4$ Hz), 13.25 (br, 1H, NH).

*Synthesis of 6-Substituted Pyrazolo[3,4-d][1,3]thiazin-4-thiones (**4a**−**j**).* The pertinent 6-substituted pyrazolo[3,4-*d*][1,3]thiazin-4-one **3a**−**j** (2 mmol) and phosphorus pentasulfide (0.49 g, 2.2 mmol) were vigorously refluxed under stirring in anhydrous xylene (24 mL) for 7 h. After cooling, the precipitate was collected and purified by column chromatography.

By using this procedure the following compounds were obtained:

4a *(R = 3-trifluoromethylphenyl):* yield, 45%; mp, 285−287 °C (purified by column chromatography; eluent ethyl acetate/petroleum ether, 1:1); IR (KBr, cm^{-1}), ν_{max} 3083, 1552, 1489; ^1H NMR (DMSO-d_6), δ 7.48−8.02 (m, 4H, Ph), 8.16 (s, 1H, CH), 11.02 (br, 1H, NH), 13.83 (br, 1H, NH).

4b *(R = 4-bromophenyl):* yield, 55%; mp, 298−300 °C (purified by column chromatography, eluent ethyl acetate:/petroleum ether, 3:7); IR (KBr, cm^{-1}), ν_{max} 3051, 1562, 1487; ^1H NMR (DMSO-d_6), δ 7.56−7.73 (m, 4H, Ph), 8.10 (s, 1H, CH), 10.87 (br, 1H, NH), 13.76 (br, 1H, NH).

4c *(R = 4-chlorophenyl):* yield, 55%; mp, 158−162 °C (purified by column chromatography, eluent ethyl acetate:/petroleum ether 3:7); IR (KBr, cm^{-1}), ν_{max} 2917, 1560, 1491; ^1H NMR (DMSO-d_6), δ 7.44−7.78 (m, 4H, Ph), 8.10 (s, 1H, CH), 10.88 (br, 1H, NH), 13.77 (br, 1H, NH).

4d *(R = 3-chlorophenyl):* yield, 35%; mp, 215−219 °C (purified by column chromatography, eluent ethyl acetate/petroleum ether: 2:8); IR (KBr, cm^{-1}), ν_{max} 2918, 1598, 1560, 1492; ^1H NMR (DMSO-d_6), δ 7.20−7.97 (m, 4H, Ph), 7.98 (s, 1H, CH), 10.89 (br, 1H, NH), 13.83 (br, 1H, NH).

4e *(R = 2-chlorophenyl):* yield, 35%; mp, 162−167 °C (purified by column chromatography; eluent ethyl acetate/petroleum ether 3:7, 8:2); IR (KBr, cm^{-1}), ν_{max} 3319, 1562, 1539, 1496; ^1H NMR (DMSO-d_6), δ 7.36−7.62 (m, 4H, Ph), 8.07 (s, 1H, CH), 10.72 (br, 1H, NH), 13.60 (br, 1H, NH).

4g *(R = ethyl):* yield, 70%; mp, 109−112 °C (purified by column chromatography, eluent ethyl acetate/petroleum ether 1:1); IR (KBr, cm^{-1}), ν_{max} 3207, 3279, 1560; ^1H NMR (DMSO-d_6), δ 1.16 (t, 3H, Me, $J = 7.2$ Hz), 3.37−3.44 (m, 2H, CH_2), 8.01 (s, 1H, CH), 8.94 (br, 1H, NH), 12.40 (v br, 1H, NH).

4h *(R = butyl):* yield, 77%; mp, 193.2 °C (purified by flash column chromatography; eluent ethyl acetate/petroleum ether 2:8, 1:1); IR (KBr, cm^{-1}), ν_{max} 3173, 2905, 1558, 1530; ^1H NMR (DMSO-d_6), δ 0.90 (t,

3H, Me, $J = 7.2$ Hz), 1.23−1.62 (m, 4H, $2CH_2$), 3.33−3.39 (m, 2H, CH_2), 8.01 (s, 1H, CH), 8.92 (br, 1H, NH), 13.44 (br, 1H, NH).

4i *(R = benzyl):* yield, 83%; mp, 195−198 °C (purified by column chromatography; eluent ethyl acetate/petroleum ether 3:7); IR (KBr, cm^{-1}), ν_{max} 3182, 1576, 1554; ^1H NMR (DMSO-d_6), δ 4.63(d, 2H, CH_2, $J = 5.4$ Hz), 7.21−7.45 (m, 5H, Ph), 8.03 (s, 1H, CH), 9.42 (br, 1H, NH), 13.50 (br, 1H, NH).

4j *(R = cyclohexyl):* yield, 34%; mp, 193−196 °C (purified by flash column chromatography; eluent ethyl acetate/petroleum ether 3:7); IR (KBr, cm^{-1}), ν_{max} 3223, 2927, 1554, 1487; ^1H NMR (DMSO-d_6), δ 1.15−2.15 (m, 10H, cyclohexyl), 4.17 (m, 1H, cyclohexyl), 7.98 (s, 1H, CH), 8.93 (br d, 1H, NH), 13.43 (br, 1H, NH).

Biological Tests. *Evaluation of Pyrazole Derivatives as Inhibitors of the Photosynthetic Electron Transport by the Hill Reaction.* Photosynthetically active thylakoid membranes were isolated from market spinach (*Spinacea oleracea* L.) leaves. Deveined plant material was resuspended in 5 mL g^{-1} of ice-cold 20 mM *N*-tris(hydroxymethyl)-methylglycine (Tricine)−NaOH buffer (pH 8.0) containing 10 mM NaCl, 5 mM $MgCl_2$, and 0.4 M sucrose and homogenized for 30 s in a blender at maximal speed. The homogenate was filtered through surgical gauze, and the filtrate was centrifuged at 4 °C for 1 min at 500*g*; the supernatant was further centrifuged for 10 min at 1500*g*. Pelleted chloroplasts were osmotically swollen by resuspension in sucrose-lacking buffer. The suspension was immediately diluted 1:1 with sucrose-containing buffer, kept on ice in the dark, and used within a few hours from the preparation. Following proper dilution with 80% (v/v) acetone, the absorbance of each sample was determined at 645 and 663 nm, and the chlorophyll content was calculated on the basis of Arnon's formula. The rate of photosynthetic electron transport was measured by the following light-driven ferricyanide reduction. Aliquots of membrane preparations corresponding to 20 μg of chlorophyll were incubated at 24 °C in 1-mL cuvettes containing 20 mM Tricine−NaOH buffer (pH 8.0), 10 mM NaCl, 5 mM $MgCl_2$, 0.2 M sucrose, and 1 mM $K_3Fe(CN)_6$. The assay was initiated by exposure to saturating light (800 μmol m^{-2} s^{-1}), and the rate of ferricyanide reduction was measured at 30-s intervals for 10 min against an exact blank at 420 nm. Activity was calculated over the linear portion of the curve from a molar extinction coefficient of 1000 M^{-1} cm^{-1}. Under the adopted conditions, the value for untreated controls was 65.8 ± 2.0 nmol of ferricyanide reduced s^{-1} (mg of chlorophyll)$^{-1}$. Pyrazole derivatives were dissolved in 0.1 M NaOH, and then the pH was brought to a value ranging from 8.0 to 8.5 with 1 M HCl; when appropriate, the solutions were further diluted with water. Their effect upon oxygen evolution was evaluated in parallel assays in which the compounds were added to the reaction mixture at concentrations ranging from 100 nM to 1 mM. Each dose was carried out at least in triplicate, and results were expressed as percentage of untreated controls. Reference herbicides were initially dissolved in water (hexazinone and lenacil) or acetone (diuron) and then water-diluted; in the case of the latter compound, controls received the same amounts of solvent. The concentrations causing 50% inhibition (IC_{50}) of in vitro activity were estimated utilizing the linear regression equation of activity values plotted against the logarithm of inhibitor concentration. At least four doses in the inhibitory range were considered. Confidence limits were computed according to the method of Snedecor and Cochran (*18*).

Molecular Modeling and Analysis of Structure−Activity Relationship. The Cambridge Structural Database (CSD) search (version 5.25, November 2003; update July 3, 2004) and structure retrieval was run on a PC working under Windows XP by the software CONQUEST (version 1.6) (*19*, *20*). All of the conformational and modeling studies were carried out on SGI-OCTANE and -R-5000 O2 workstations operating under IRIX 6.5.+ using the software Macromodel (version 8.1) as implemented in the version 5.1 of the MAESTRO suite (*21*, *22*), SPARTAN (version 2002) (*23*), and HINT2.35S (*24*) as implemented in SYBYL 6.9 (*25*). During the review process a new version of SYBYL (7.0 update 1), comprehensive of the new HINT 3.09S, was released. Provided that nothing is conceptually changed, slight numerical differences can be registered with respect to the HINT log *P* values reported in this paper.

The CSD files of dimethyl-1-(3-chloro-4-methylphenyl)pyrazole-3,4-dicarboxylate (database entry: BANQUD) and 4-cyano-3-(4-methoxyphenyl)-1-phenylpyrazole (database entry: BIRFOX) were exported to .mol2 files, read, and modified by the fragment library in the software MACROMODEL (version. 8.1) as implemented in the MAESTRO suite (*21*, *22*) and used as the building blocks for compounds **1**−**4**, whereas the atrazine structure as extracted from the pdb entry 1DXR was used as the building block for compounds **5** and **6**. After each export, the atom potential types and bond orders were carefully checked to evaluate their correctness with respect to the intended structure prior to the Macromodel (*21*, *22*), SPARTAN (*23*), and HINT (*24*) sessions (e.g., compound **3f**, where the NO_2 needed to be set in SPARTAN as dianionic). The .mol2 files were saved as .prj files for MACROMODEL, and a minimization (2000 steps, convergence 0.001) was carried out using the default static Merck Molecular Force Field as implemented in MACROMODEL 8.1 (*21*, *22*). Default options were used with the Polak-Ribiere Conjugate Gradient scheme, until a gradient of 0.001 kcal $Å^{-1}$ was reached. To search the conformational space, 2000MC steps were performed on each starting conformation. Least-squares superposition of all non-hydrogen atoms was used to eliminate duplicate conformations. An energy cutoff of 12.5 kcal mol^{-1} (50.0 kJ mol^{-1}), high enough to map the conformational space of these rigid molecules including the bioactive conformation, was applied to the search results. Aqueous and in vacuo conformational analyses were performed using the Monte Carlo Multiple Minimum Search protocol as implemented in the MACROMODEL (*21*, *22*) software. Because in the Monte Carlo approach the dynamic of a molecule is simulated by randomly changing dihedral angle rotations or atom positions, the trial conformation is accepted if its energy has decreased from the previous one. If the energy level is higher, there are various criteria to select the calculated conformer or not. In our simulations, all of the dihedral angles of single linear bonds were allowed to move freely, and the conformation was accepted if the energy was lower than that of the previous conformation or within a fixed energy window as selector. The lowest energy conformers were further optimized using the multiple minimization protocol as implemented in MACROMODEL 8.1 (*21*, *22*). The minima were exported to .mol2 and saved as .spinput files for the SPARTAN (log Ps and electrostatic potential calculations) using the semiempirical model RHF/PM3/MMFF94s as in SPARTAN (*23*). Slightly different values but a similar trend were obtained using the semiempirical model RHF/AM1/MMFF94s as in SPARTAN (*23*). Compound (**2p**) was calculated in its negatively charged (carboxylate) form, assuming it was similar to that in the biological medium. Electrostatic potential ramp (kcal/mol) was observed to change from red (more negative values) to blue (higher values). The .mol2 files were used as such for the HINT (log *P* calculations and hydropathicity maps) (*24*) calculations, for which all of the HINT settings were left as default.

RESULTS AND DISCUSSION

Synthesis. The preparative route to the target products **3a**−**j** and **4a**−**j** is outlined in **Scheme 2**. *N*-Alkyl/aryl-*N*′-(4-carboethoxy-3-pyrazolyl)thioureas **8** were obtained by reaction of 3-amino-4-carboethoxypyrazole **7** with the appropriate isothiocyanate. High yields of **8** have been obtained in the reaction of **7** with arylisothiocyanates, but, in the reaction of **7** with ethyl, butyl, and cyclohexyl isothiocyanate, the *N*′-(3-pyrazolyl)-thioureas **8g**,**h**,**j** were isolated after purification by silica gel chromatography as byproducts. Cyclization of **8** with 98% sulfuric acid provided the required 6-substituted pyrazolo-[3,4-*d*][1,3]thiazin-4-ones **3**. Thiation of **3** with P_2S_5 gave the corresponding 6-substituted pyrazolo-[3,4-*d*][1,3]thiazin-4-thiones **4**.

Biological Activity. 4-Carboxypyrazolo-3-*tert*-butylcarboxamide and 4-carboxypyrazolo-3-cyclopropylcarboxamide derivatives (**1** and **2**) were synthesized on the basis of results previously described, concerning the biological activity of isoxazoledicarboxylic acid derivatives (*9*). Among the compounds tested in that study, some 4-carboxyisoxazole-3-carboxamides had been reported as potent inhibitors of the photosynthetic electron transport at the PSII level, with IC_{50}

Scheme 2

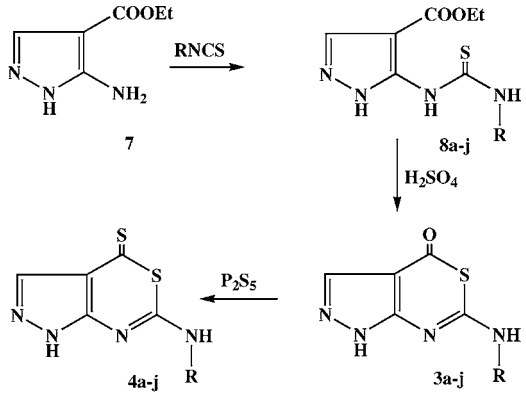

values ranging from 0.3 to 30 μM. In fact, the reference compounds 4-carboxyisoxazole-3-isopropylcarboxamide (**2m**) and 4-carboxyisoxazole-3-*tert*-butylcarboxamide (**1m**) were found to interfere with the light-driven ferricyanide reduction by isolated spinach thylakoids. Under the experimental conditions employed, they showed a lower efficiency, with IC_{50} values of 100 and 290 μM, respectively (**Table 1**). Nevertheless, the replacement of the carboxyisoxazole moiety with a carboxypyrazole (as in compound **2s**) resulted in a loss of activity. Interestingly, however, the insertion of substituents in position 1 restored at least in part the ability to interfere with the Hill reaction. The methyl (**1n** and **2n**) and *p*-chlorophenyl (**1q** and **2q**) derivatives showed maximal activity, with IC_{50} values ranging from 0.4 to 1.2 mM, whereas the presence of a *tert*-butyl substituent (**1o** and **2o**) was ineffective (**Table 1**). Due to the higher concentration needed for Hill reaction inhibition, these compounds seem not to be satisfactory for use as agrochemicals.

More promising results were obtained with the other two groups of pyrazole derivatives. In previous work, we described the features of a few pyrazolo[1,5-*a*][1,3,5]triazine-2,4-dione (**5**) and pyrazolo[1,5-*c*][1,3,5]thiadiazine-2-one (**6**) derivatives, some of which showed excellent in vitro inhibitory activity against the PSII, comparable to those of commercial reference herbicides (*14*). The potential of a number of new pyrazolo-[3,4-*d*][1,3]thiazine-4-ones and pyrazolo[3,4-*d*][1,3]thiazine-4-thiones was then investigated. All compounds tested were found to inhibit ferricyanide reduction by spinach thylakoid membranes, with IC_{50} values ranging in most cases from 10^{-6} to 10^{-4} M (**Tables 2** and **3**). As to the analysis of the scaffold effect (thiazine-4-one versus thiazine-4-thione), the comparison between compounds that have exactly the same substituents strongly suggested that the replacement of the oxygen moiety with sulfur acts to amplify the inhibitory effect. In general, the IC_{50} for a given pyrazolo[3,4-*d*][1,3]thiazine-4-thione (**Table 3**) was, in fact, 2−100-fold lower than that of its thiazine-4-one counterpart (**Table 2**). In the latter group, maximal activity was shown by the compound bearing the benzyl substituent (**3i**), with an IC_{50} of 11 μM. Among thiazine-4-thiones, more than half of the compounds (**4a**,**b**,**h**−**j**) showed IC_{50} values lower than 10 μM, and maximal efficacy was related to the presence of a cyclohexyl substituent (**4j**). The efficacy of **4j** in inhibiting the Hill reaction (IC_{50} = 0.64 μM) is comparable to those

Table 1. In Vitro Effects of 4-Carboxypyrazolo-3-*tert*-butylcarboxamide and 4-Carboxypyrazolo-3-cyclopropylcarboxamide Derivatives on Ferricyanide Reduction by Functionally Intact Chloroplasts Isolated from *S. oleracea* Leaves[a]

Compound	R	IC_{50}[b] (mM)	pIC_{50} (M)
1n	—CH_3	0.67 ± 0.11	3.174
1o	—$C(CH_3)_3$	> 100	<1.000
1p	—C_6H_5	7.60 ± 1.53	2.119
1q	—C_6H_4-Cl	0.95 ± 0.14	3.022
1r	—C_6H_3Cl-CF_3	1.04 ± 0.09	2.983
2n	—CH_3	1.19 ± 0.41	2.924
2o	—$C(CH_3)_3$	68 ± 22	1.167
2p	—C_6H_5	22.5 ± 14.3	1.648
2q	—C_6H_4-Cl	0.37 ± 0.04	3.432
2r	—C_6H_3Cl-CF_3	12.2 ± 3.9	1.914
2s	—H	> 100	<1.000
1m		0.10 ± 0.01	4.000
2m		0.29 ± 0.04	3.538

[a] Activity was measured as described under Materials and Methods either in the absence or in the presence of pyrazole derivatives at concentrations ranging from 30 μM to 1 mM. Each sample was carried out at least in triplicate, and values were expressed as percentage of untreated controls. [b] The concentrations causing 50% inhibition (IC_{50}) of in vitro activity were estimated as described under Materials and Methods utilizing the linear regression equation of the activity values plotted against the logarithm of inhibitor concentration. Confidence limits were computed according to the method of Snedecor and Cochran (*18*).

previously found (*14*) for commercial herbicides, such as diuron, lenacil, and hexazinone (IC_{50} = 0.27, 0.08 and 0.11 μM, respectively). The positive effect of the sulfur moiety might be interpreted as a function of the corresponding increase in lipophilicity. However, this may not be the case, because lipophilicity does not appear to be a general descriptor of the activity (vide infra). Alternatively, a slightly different target might be supposed for each chemotype.

Because the method employed, which measures the reduction of an electron acceptor (the ferricyanide) downstream from PSI, does not distinguish the exact target in the electron transport chain, further trials were performed with the two most active compounds (**4j** and **3i**) by the addition of 2 μM 2,5-dibromo-3-methyl-6-isopropyl-*p*-benzoquinone, a cytochrome b_6f inhibitor. The subsequent inclusion in the reaction mixture of 0.1 mM phenylenediamine restored electron transfer from water to ferricyanide that excludes PSI. The ability of **4j** and **3i** to inhibit this transfer at similar rates (data not shown) indicated that PSI is not involved and that, as expected and previously determined for compounds **5** and **6** (*14*), PSII is the target of their action.

Structure−Activity Relationships. An analysis of structural requirements for the inhibitory activity against PSII was then performed, including data previously obtained in the case of the pyrazolo[1,5-*a*][1,3,5]triazine-2,4-dione and pyrazolo[1,5-*c*][1,3,5]thiadiazine-2-one derivatives **5** and **6** (*14*; **Table 4**). Compounds **1o**, **2o**, **2p**, **2r**, **3f**, **3h**, **4a**, **4h**, **5e**, **5h**, **5j**, **6h**, and **6j**, spanning a range of >6 orders of magnitude (from active to inactive), were selected. Most of them are not conformationally flexible, and only a few derivatives in the active series show

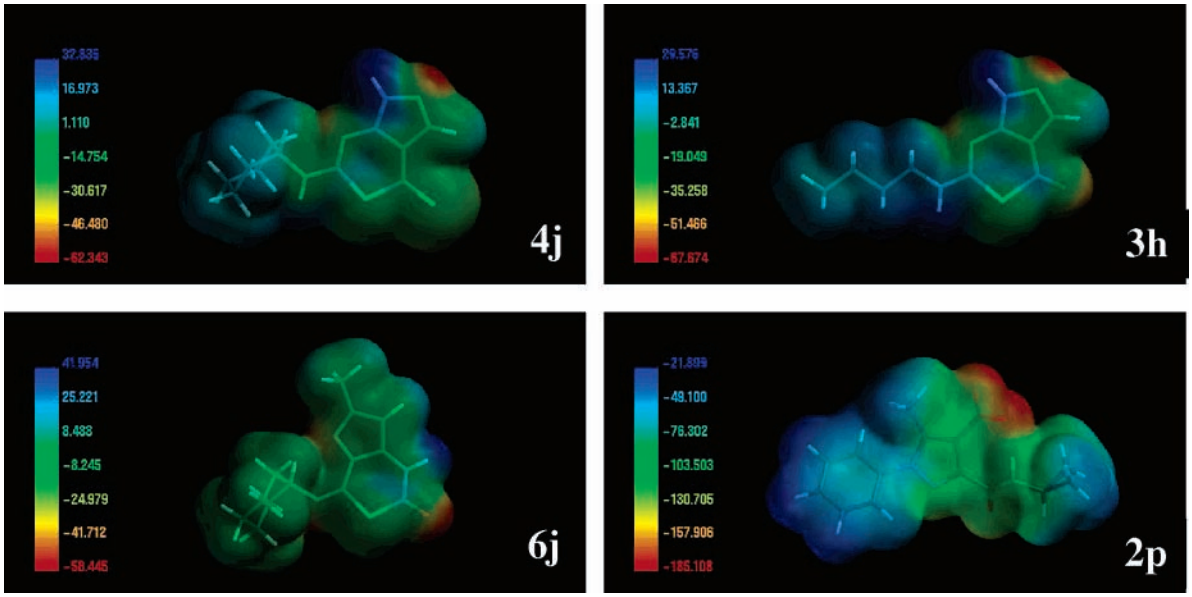

Figure 1. SPARTAN 02 transparent electrostatic surface maps of active (**4j** and **6j**) versus less active (**3h**) and inactive (**2p**) compounds. Effective molecules in the investigated series (tube representation) have a positive electrostatic surface [**4j**, from –62.343 (red) to 32.835 (blue); **6j**, from –58.445 (red) to 41.954 (blue)] as a common motif, whereas the ineffective compound **2p** (tube representation as carboxylate, see text) shows a strong negative surface [from –185.108 (red) to –21.899 (blue)]. The moderately active compound **3h** [from –57.674 (red) to 29.576 (blue)] presents an intermediate electrostatic character. Electrostatic potentials are in kcal/mol. E-plot values are expressed as e/au^3.

Table 2. In Vitro Effects of Pyrazolo[3,4-*d*][1,3]thiazine-4-one Derivatives on Ferricyanide Reduction by Photosynthetically Active Thylakoid Membranes Isolated from *S. oleracea*[a]

Compound	R	IC_{50} [b] (μM)	pIC_{50} (M)
3a		33.2 ± 13.4	4.479
3b	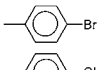	28.5 ± 6.4	4.545
3c		38.5 ± 4.6	4.415
3d		48.0 ± 6.4	4.319
3e		47.8 ± 19.0	4.321
3f	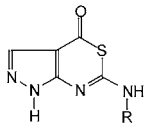 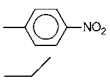	1056 ± 398	2.976
3g		335 ± 65	3.475
3h		211 ± 62	3.676
3i		10.8 ± 3.1	4.967
3j		66.5 ± 22.5	4.177

[a] Activity was measured as described under Materials and Methods either in the absence or in the presence of pyrazole derivatives at concentrations ranging from 1 μM to 1 mM. Each sample was carried out at least in triplicate, and values were expressed as percentage of untreated controls. [b] The concentrations causing 50% inhibition (IC_{50}) of in vitro activity were estimated as described under Materials and Methods utilizing the linear regression equation of the activity values plotted against the logarithm of inhibitor concentration. Confidence limits were computed according to the method of Snedecor and Cochran (*18*).

Table 3. In Vitro Effects of Pyrazolo[3,4-*d*][1,3]thiazine-4-thione Derivatives on the Hill Reaction by Functional Chloroplasts Isolated from *S. oleracea* Leaves[a]

Compound	R	IC_{50} [b] (μM)	pIC_{50} (M)
4a		2.78 ± 0.57	5.556
4b	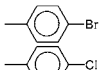	6.06 ± 1.06	5.218
4c	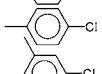	21.3 ± 6.4	4.672
4d		15.3 ± 4.2	4.815
4e		43.1 ± 13.5	4.366
4g	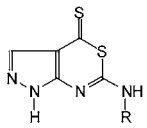 	10.7 ± 1.2	4.971
4h		2.67 ± 0.20	5.573
4i		2.84 ± 0.44	5.547
4j		0.64 ± 0.13	6.194

[a] Activity was measured as described under Materials and Methods either in the absence or in the presence of pyrazole derivatives at concentrations ranging from 0.1 μM to 0.1 mM. Each sample was carried out at least in triplicate, and values were expressed as percentage of untreated controls. [b] The concentrations causing 50% inhibition (IC_{50}) of in vitro activity were estimated as described under Materials and Methods utilizing the linear regression equation of the activity values plotted against the logarithm of inhibitor concentration. Confidence limits were computed according to the method of Snedecor and Cochran (*18*).

some degree of conformational freedom, thus making each analysis straightforward. SPARTAN log Ps were counterchecked by both of the implemented methods in the SPARTAN 02 suite [Ghose-Crippen (*26*) and Villar (*27*, *28*)], which imply that the hydrophobicity of a molecule can be obtained as the sum of certain atomic contributions. The former is an atom-based approach, in which each atom of the molecules is assigned to a particular class, with additive contributions to the total value of log *P* and molar refractivity, whereas the latter is based on a quantum mechanical parametrization of a conformationally dependent hydrophobicity index. The values obtained showed a similar trend (data not shown), although—as expected—they were numerically different due to the different paradigms underlying the calculation. The Ghose–Crippen model is parametrized for 110 atom types, including common bondings of H, C, N, O, S, and the halogens. For a test suite of 494 molecules, it gives a standard deviation of 0.347 and a correlated coefficient of 0.962. In a test suite of 69 compounds beyond the original one, it predicts a variance of 0.404. Villar is a model

Table 4. In Vitro Effects of Some Commercial PSII-Inhibiting Herbicides, Pyrazolo[1,5-*a*][1,3,5]triazine-2,4-dione, and pyrazolo[1,5-*c*][1,3,5]thiadiazine-2-one Derivatives on Light-Driven Ferricyanide Reduction by Functionally Intact *S. oleracea* Chloroplasts[a]

Compound	R	pIC_{50} (M)
Diuron	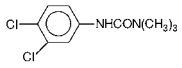	6.569
Hexazinone	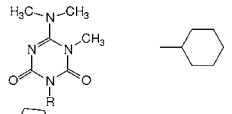	6.959
Lenacil	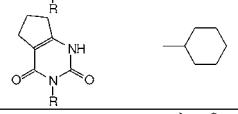	7.097
5e		5.585
5g	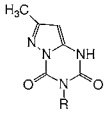	4.495
5h		5.180
5i		4.377
5j		6.495
5l		3.772
6g	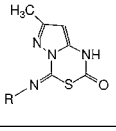	5.538
6h		6.244
6i		4.745
6j		6.678

[a] Data obtained by replotting previously reported results (*14*).

that works only on semiempirical wave functions with no d orbitals. The Villar method examines the overlap matrix, searching for the type and number of lone pairs as well as the surface area of each atom. It is parametrized for H, C, N, O, F, S, and Cl (*23*, *27*, *28*).

The same trend was observed for the HINT log Ps. HINT is a novel empirical molecular modeling system that translates the well-developed Medicinal Chemistry and QSAR formalism of Log *P* and hydrophobicity into a free energy interaction model for all biomolecular systems based on the experimental data from solvent partitioning. HINT calculates three-dimensional hydropathic interaction maps that are uniquely instructive for understanding biomacromolecular structure: substrate/inhibitor/drug binding to proteins and nucleotides, protein subunit interactions, and protein folding. The hydrophobic atom constants are calculated using an adaptation of the fragment constant methods of Leo and Rekker (*24*, *29*, *30*). The partition constant, Log *P*, is a thermodynamic parameter that, because of its unprocessed and unbiased experimental nature, contains interaction information specific to the biological environment as well as solvent effects and entropy. In other terms, it encodes all significant intermolecular and intramolecular non-covalent interactions implicated in drug binding or protein folding. Two types of output data are generated by HINT: tabular lists of specific atom−atom interactions quantitated by a microinteraction constant and a variety of graphical maps that reveal (1) hydropathy, (2) hydropathic interactions, and (3) hydropathy of an unknown, inferred complementary species (e.g., to design a substrate to fit a known receptor).

By means of such an approach a good relationship was found between the electrostatic properties of the molecules and their activity. All of the active molecules in the investigated series show a highly positive electrostatic potential as a common motif, whereas, according to previous studies (*10*), inactive compounds share strong negative areas (**Figure 1**). Moderately active

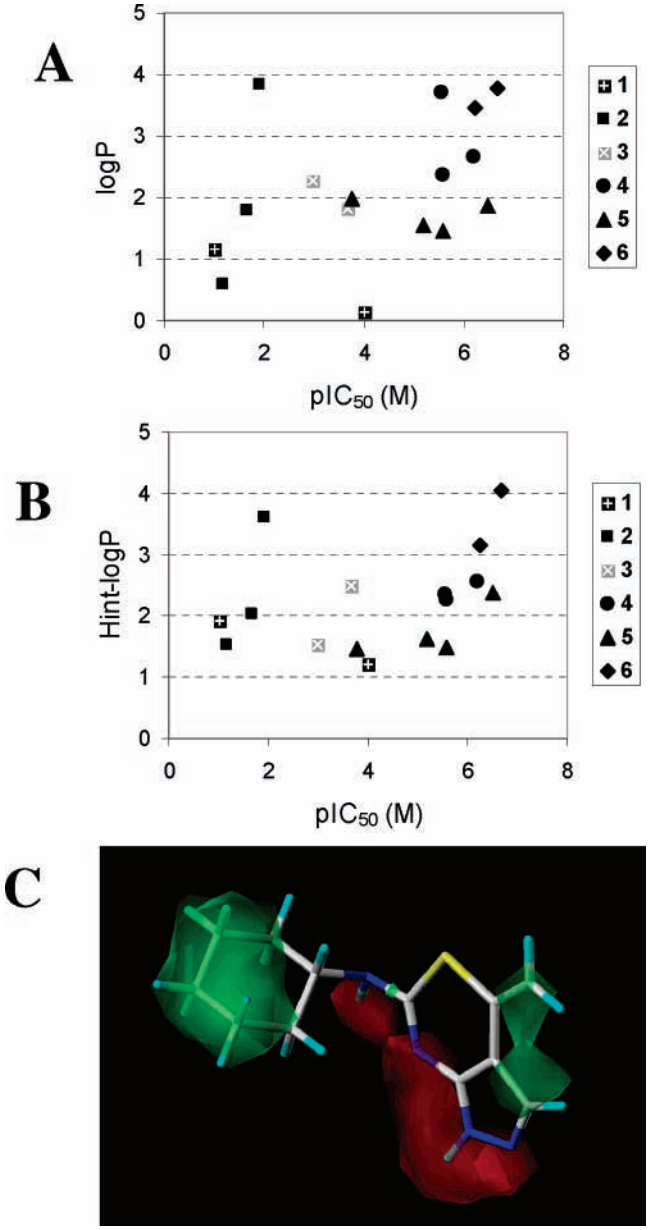

Figure 2. Partition coefficients (log Ps) of selected compounds as related to their biological activity. Similar trends were obtained with either the methods in the SPARTAN 02 suite (Ghose–Crippen and Villar) (**A**) or HINT-log *P* (**B**) values. A HINT transparent hydropatic map of the active compound **4j** (stick representation) is also shown (**C**): red contours indicate polar regions, and green contours indicate hydrophobic regions.

compounds show an intermediate electrostatic character, thus strengthening the conclusion. If the electrostatic potential may represent to some extent a discriminant factor between active and inactive series/compounds, the same seems to be untrue for lipophilicity. Hydropathic interaction indices were found to be related to the biological activity within the same series, but did not discriminate between different series (**Figure 2A**), because some inactive compounds in series **1** and **2** showed log *P* values comparable to those of active compounds in series **4** and **5**. Also three-dimensional HINT (hydropatic) maps, which are based on log *P* constants, are consistent with this trend (**Figure 2B**,**C**). Further QSAR and modeling studies combining different computational approaches are currently in progress to define a pharmacophoric pattern, aiming at the synthesis of more active chemotypes.

ACKNOWLEDGMENT

We thank Dr. Eva Segato for skillful technical assistance. We gratefully acknowledge Prof. Pietro Cozzini (Molecular Modeling Laboratory, Department of General and Inorganic Chemistry, University of Parma) and Wavefunction, Inc., for helpful discussions and suggestions.

LITERATURE CITED

(1) Heap, I. International survey of herbicide resistant weeds, http://www.weedscience.org, accessed Dec 28, 2004.
(2) Devine, M. D.; Shukla, A. Altered target sites as a mechanism of herbicide resistance. *Crop Prot.* **2000**, *19*, 881−889.
(3) Oettmeier, W. Herbicide resistance and supersensitivity in photosystem II. *Cell. Mol. Life Sci.* **1999**, *55*, 1255−1277.
(4) Wakabayashi, K.; Boger, P. Target sites for herbicides: entering the 21st century. *Pest Manag. Sci.* **2002**, *58*, 1149−1154.
(5) Lein, W.; Bornke, F.; Reindl, A.; Ehrhardt, T.; Stitt, M.; Sonnewald, U. Target-based discovery of novel herbicides. *Curr. Opin. Plant Biol.* **2004**, *7*, 219−225.
(6) Schmidt, R. R. HRAC classification of herbicides according to mode of action. *Brighton Crop Prot. Conf.−Weeds* **1997**, 1133−1140 (http://www.weedscience.org/summary/ChemFamilySum.asp?lstActive=&lstHRAC=&btnSub2=Go).
(7) Hess, F. D. Light-dependent herbicides: an overview. *Weed Sci.* **2000**, *48*, 160−170.
(8) Rutherford, A. W.; Krieger-Liszkay, A. Herbicide-induced oxidative stress in photosystem II. *Trends Biochem. Sci.* **2001**, *26*, 648−653.
(9) Münster, P.; Freund, W.; Maywald, V.; Kükenhöhner, T.; Gerber, M.; Grossmann, K.; Walter, H. Synthesis and herbicidal activity of isoxazoledicarboxylic acid derivatives. *Pestic. Sci.* **1995**, *44*, 21−27.
(10) Dayan, F. E.; Vincent, A. C.; Romagni, J. G.; Allen, S. N.; Duke, S. O.; Duke, M. V.; Bowling, J. J.; Zjawiony, J. K. Amino- and urea-substituted thiazoles inhibit photosynthetic electron transfer. *J. Agric. Food Chem.* **2000**, *48*, 3689−3693.
(11) Jewess, P. J.; Higgins, J.; Berry, K. J.; Moss, S. R.; Boogaard, A. B.; Khambay, B. P. Herbicidal action of 2-hydroxy-3-alkyl-1,4-naphthoquinones. *Pest Manag. Sci.* **2002**, *58*, 234−242.
(12) Wang, Q.; Sun, H.; Cao, H.; Cheng, M.; Huang, R. Synthesis and herbicidal activity of 2-cyano-3-substituted-pyridinemethylaminoacrylates. *J. Agric. Food Chem.* **2003**, *51*, 5030−5035.
(13) Wang, Q.; Li, H.; Li, Y.; Huang, R. Synthesis and herbicidal activity of 2-cyano-3-(2-chlorothiazol-5-yl)methylaminoacrylates. *J. Agric. Food Chem.* **2004**, *52*, 1918−1922.
(14) Vicentini, C. B.; Mares, D.; Tartari, A.; Manfrini, M.; Forlani, G. Synthesis of pyrazole derivatives and their evaluation as photosynthetic electron transport inhibitors. *J. Agric. Food Chem.* **2004**, *52*, 1898−1906.
(15) Ferreira, K. N.; Iverson, T. M.; Maghlaoui, K.; Barber, J.; Iwata, S. Architecture of the photosynthetic oxygen-evolving center. *Science* **2004**, *303*, 1831−1838.
(16) Veronese, A. C.; Callegari, R.; Morelli, C. F.; Vicentini, C. B. A facile synthesis of pyrazole, isoxazole and pyrimidine orthodicarboxylic acid derivatives via β-enaminoketoesters. *Tetrahedron* **1997**, *42*, 14497−14506.
(17) Vicentini, C. B.; Mazzanti, M.; Morelli, C. F.; Manfrini, M. A new synthetic entry to 3-carboxamido-4-carboxylic acid derivatives of isoxazole and pyrazole. *J. Heterocycl. Chem.* **2000**, *37*, 175−180.
(18) Snedecor, G. W.; Cochran, W. G. *Statistical Methods*, 6th ed.; The Iowa State University Press: Ames, IA, 1967; pp 159−160.
(19) Allen, F. H. The Cambridge Structural Database: a quarter of a million crystal structures and rising. *Acta Crystallogr. B* **2002**, *58*, 380−388.
(20) Bruno, I. J.; Cole, J. C.; Edgington, P. R.; Kessler, M.; Macrae, C. F.; McCabe, P.; Pearson, J.; Taylor, R. New software for searching the Cambridge Structural Database and visualising crystal structures. *Acta Crystallogr. B* **2002**, *58*, 389−397.
(21) Mohamadi, F.; Richards, N. G. J.; Guida, W. C.; Liskamp, R.; Lipton, M.; Caufield, C.; Chang, G.; Hendrickson, T.; Still, W. C. MacroModel−An integrated software system for modeling organic and bioorganic molecules using molecular mechanics. *J. Comput. Chem.* **1990**, *11*, 440−467.
(22) Schrodinger, Inc. http://www.schrodinger.com.
(23) SPARTAN '02, Wavefunction, Inc.http://www.wavefun.com.
(24) Kellogg, G. E.; Abraham, D. J. Is $LogP_{o/w}$ more than the sum of its parts? *Eur. J. Med. Chem.* **2000**, *35*, 651−661, and references cited therein.
(25) SYBYL Molecular Modelling Software, version 6.9; Tripos Inc. http://www.tripos.com.
(26) Ghose, A. K.; Pritchett, A.; Crippen, G. M. Atomic physicochemical parameters for three-dimensional-structure-directed quantitative structure−activity relationships. 3. Modeling hydrophobic interactions. *J. Comput. Chem.* **1988**, *9*, 80−90.
(27) Alkorta, I.; Villar, H. O. Quantum mechanical parametrization of a conformationally dependent hydrophobic index. *Int. J. Quantum Chem.* **1992**, *44*, 203−218.
(28) Kantola, A.; Villar, H. O.; Loew, G. H. Atom-based parametrization for a conformationally dependent hydrophobic index. *J. Comput. Chem.* **1991**, *12*, 681−689.
(29) Hansch, C.; Leo, A. *Substituent Constants for Correlation Analysis in Chemistry and Biology*; Wiley: New York, 1979.
(30) Abraham, D. J.; Leo, A. J. Hydrophobicity (delta G1/2 cal). *Proteins* **1987**, *2*, 130−152, and references cited therein.

Received for review January 2, 2005. Revised manuscript received March 16, 2005. Accepted March 16, 2005. This work was supported by grants from Ministero dell'Università e della Ricerca Scientifica e Tecnologica (MURST) of Italy.

JF0500029